RSC Advances

ROYAL SOCIETY OF CHEMISTRY

www.rsc.org/advances

Journal Name

RSCPublishing

COMMUNICATION

Diindeno[1,2-*g*:1',2'-*s*]rubicene: all-carbon non-fullerene electron acceptor for efficient bulk-heterojunction organic solar cells with high open-circuit voltage

Cite this: DOI: 10.1039/x0xx00000x

Received ooth January 2012,
Accepted ooth January 2012

DOI: 10.1039/x0xx00000x

www.rsc.org/

Hung-Yang Chen,[a] Jan Golder,[a] Shih-Chieh Yeh,[a] Chiao-Wen Lin,[a] Chao-Tsen Chen*[b] and Chin-Ti Chen*[a]

An all carbon non-fullerene electron acceptor material based on diindeno[1,2-*g*:1',2'-*s*]rubicene (DIR) was readily synthesized and processed for bulk-heterojunction organic solar cells. High PCE up to 3.05% with a relatively high V_{OC} of 1.22 V has been achieved with P3HT electron donor material by the variation of donor-acceptor blending ratio.

Extensive efforts have been directed toward the research of solution processed bulk heterojunction (BHJ) organic solar cells (OSCs) due to its potential for low-cost energy harvesting and large area fabrication. Power conversion efficiencies (PCEs) have already exceeded 10% for BHJ OSCs employing the π-conjugated polymer[1] or small molecule[2] as electron donors when fullerene derivatives were utilized as the electron acceptor. Large electron affinity, high electron mobility through three-dimensional charge transport and desirable phase separation in the BHJ active layer are major advantages of fullerene derivatives as dominant electron acceptor materials for highly efficient BHJ OSCs.[3] However, some obvious drawbacks of fullerene acceptors limited their practical usages in BHJ OSCs, such as a non-trivial matter of synthesis and purification,[4] insufficient solubility in processing solvent. Moreover, the poor absorption in the visible wavelength and relatively deep-lying lowest unoccupied molecular orbital (LUMO) energy level of fullerene acceptors resulting in photon energy losses and low open-circuit voltage (V_{OC}) of the photovoltaic device. In light of these drawbacks, non-fullerene electron acceptors based on small molecules[5,6] and polymers[7] that are readily synthesized and HOMO/LUMO energy levels tunable, as well as showing broad absorption in the visible wavelength have attracted increasing research efforts in materials development to improve the performance of BHJ OSCs.

A popular strategy for the design of non-fullerene electron acceptors is to utilize planar electron-deficient building units, such as perylene diimide (PDI),[8-13] fluoranthene-fused imide (FFI),[14] diketopyrrolopyrrole (DPP),[15] benzothiadiazole (BT),[16] and benzothiadiazole/imide.[17] Recently, the highest PCEs of BHJ OSCs using the small molecular non-fullerene acceptor based on the conventional polymer donor P3HT have already exceeded 4% by using an azadipyrromethene-based Zn complex as the acceptor.[18] Moreover, lots of effort have been directed to the development of perylene diimide (PDI)-based acceptors[8-12] recently and the highest PCE exceeded 6% has been obtained when the low-band gap polymer PBDTTT-C-T was utilized as the donor material.[13] In terms of molecular structure, fullerenes are unique because they do not contain electron-deficient building units. The electron-accepting ability of fullerenes is rationalized by recognizing that fullerenes contain cyclopentadiene rings that have the driving force to aromatize by accepting electrons through aromatic 4*n*+2 stabilizations.[19,20] Within the context, cyclopenta-fused polycyclic aromatic hydrocarbons (CP-PAHs) contain cyclopentadiene rings and behave similarly as fullerenes in exhibiting high electron affinities. Several CP-PAHs have been shown to function as *n*-type or ambipolar semiconductors in organic field-effect transistors (OFETs), such as indenofluorenes,[21] cyclopenta[*hi*]aceantrylenes,[19] dibenzopentalenes,[22] and emeraldicenes.[23] However, only few CP-PAHs have utilized as electron acceptors in BHJ OSCs.[24-27] Recently, Plunkett *et al.* demonstrated the potential of cyclepenta[*hi*]aceanthrylene (CPA) small molecules[28] and polymers[29] as electron acceptors through the fluorescence quenching study of P3HT. Miao *et al.* also utilized a CPA derivative as the cascade material that exhibits electron-accepting properties to enhance the PCE of BHJ OSCs based on a ternary blend system.[30] We were therefore encouraged by their discoveries and interested in developing electron acceptors based on CPA structure.

As a molecular fragment of C_{70}, rubicence (Scheme 1) has a low LUMO energy level of ~3.4 eV and it is a structural analogue of CPA with the potential to have fullerene-like electron affinity due to aromatic 4*n*+2 stabilizations mentioned above.[31] Herein, we report an all-carbon non-fullerene electron acceptor adopting rubicene as the core structure, which is known as diindeno[1,2-*g*:1',2'-*s*]rubicene (DIR) as shown in Scheme 1.[32]

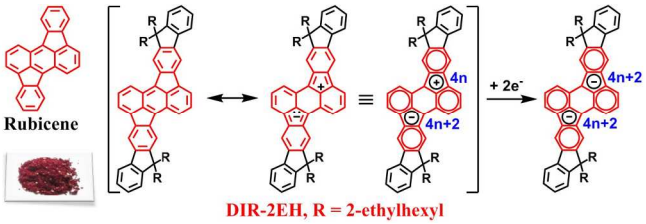

Scheme 1 Chemical structures of rubicene, DIR-2EH and the benzocyclopentadienyl anion stabilization of DIR-2EH. Inset shows the photograph of sublimed crystalline solids of DIR-2EH.

Synthetically, DIR-2EH is readily anchored with branched 2-ethylhexyl (2EH) chains in order to improve the solubility for the fabrication of solution-processed BHJ OSCs. DIR-2EH has no electronegative heteroatom but only carbon and hydrogen atoms. The synthesis of DIR-2EH was modified according to the synthetic route reported by Skidmore *et al.*[32] DIR-2EH can be easily obtained within three synthetic steps with reasonably good to high yields from the commercially available starting material 1,5-dichloroanthraquinone as shown in Scheme S1 (ESI†). To ensure the material purity required for BHJ OSCs, DIR-2EH could be readily purified by vacuum gradient sublimation after column chromatography. The sublimed crystalline solid of DIR-2EH shows a bright red colour and exhibits excellent solubility in common organic solvents like 1,2-dichloromethane, chloroform, chlorobenzene and 1,2-dichlorobenzene at room temperature.

Fig. 1 shows the UV-visible absorption spectra of DIR-2EH dissolved in 1,2-dichlorobenzene and as thin film. Owing to the four bulky 2EH chains (which prevents π-π stacking among arc-shaped structure of rubicene), comparing those in solution, absorption spectra of DIR-2EH are slightly red-shifted in thin film states. DIR-2EH shows an intense absorption band around 350 nm and a weaker but much broader absorption band with fine structures ranging from 400 to 600 nm. The absorption band of DIR-2EH in the visible wavelength corresponds to the π-π* transition of the conjugated diindeno[1,2-*g*:1',2'-*s*]rubicene structure, which has more extended π-conjugation than the parent rubicene and hence its absorption wavelength is red-shifted.[33] Based on the thin film absorption spectrum, the optical energy gap (E_g) of DIR-2EH was calculated to be 1.97 eV. Fig. 1 (right) also shows the absorption spectra of P3HT:DIR-2EH blend films, in which the material blending ratio is 1:1, 1:2 and 1:4. Whereas $PC_{61}BM$ has a strong absorption ~330 nm and a series of weak absorption bands extended beyond 550 nm, the absorption band around 350 nm for the P3HT:DIR-2EH blend films is attributed to DIR-2EH. The increasing absorption intensities at 550 nm and 600 nm, which are synchronously along with increasing blending ratios, are mainly attributed to the absorption of DIR-2EH.

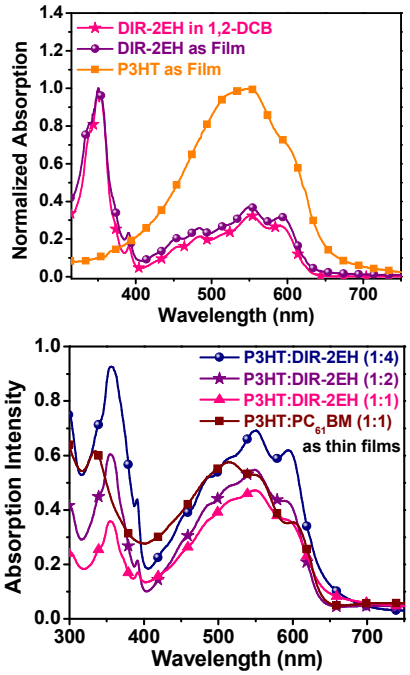

Fig. 1 Absorption spectra of DIR-2EH in 1,2-dichlorobenzene and DIR-2EH and P3HT as thin film (top); P3HT:DIR-2EH (1:1, 1:2, 1:4) and P3HT:$PC_{61}BM$ (1:1) as thin film (bottom).

The HOMO/LUMO energy levels of DIR-2EH were investigated by cyclic voltammetry (CV) method. The classical electron acceptor $PC_{61}BM$ was also measured in the same condition for comparison. The detail of CV measurement is provided in ESI†. As shown in Fig. 2, DIR-2EH exhibits two quasi-reversible reduction signals that are ascribed to the formation of two stabilized aromatic benzocyclipentadienyl anions in the rubicene core structure of DIR-2EH.[28] It can be seen that the first and second reduction potentials all shifted negatively when compared to $PC_{61}BM$. The LUMO energy level of DIR-2EH was estimated from the onset of the first reduction potential and calculated according to the onset oxidation potential of ferrocene, which is 4.8 eV below vacuum level.[27] The LUMO of DIR-2EH was estimated to be -3.30 eV, which is 0.5 eV higher than -3.80 eV of $PC_{61}BM$. It has been known that the upper limit of V_{OC} is determined by the difference of the LUMO energy level of the electron acceptor and the HOMO energy level of the electron donor. Therefore, the much higher LUMO level of DIR-2EH than $PC_{61}BM$ should theoretically lead to a much higher V_{OC} in BHJ OSCs.

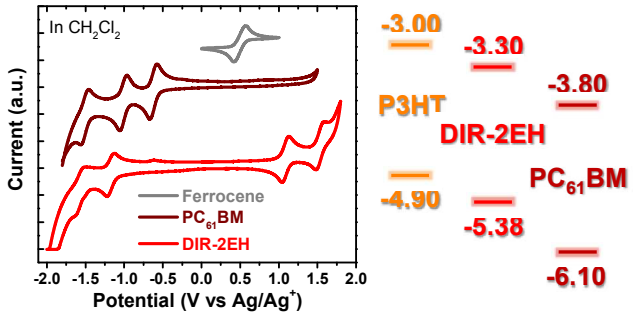

Fig. 2 Left: cyclic voltammograms of DIR-2EH and $PC_{61}BM$ in CH_2Cl_2; Right: energy levels of P3HT, $PC_{61}BM$ and DIR-2EH; the HOMO and LUMO levels of P3HT was taken from the literature, which was obtained from cyclic voltammetry.[34]

The photoluminescence (PL) quenching of the electron donor in the presence of the electron acceptor is a typical characteristic of electron transfer from donor material to acceptor material. We performed PL quenching study of P3HT in solution (chloroform) containing DIR-2EH with varying (see Fig. S1 in ESI†). The PL intensity of P3HT solution decreased dramatically with increasing concentrations of DIR-2EH. We further utilized the Stern-Volmer quenching plot to investigate the quenching efficiency of DIR-2EH (Fig. S1). From the plot, a quenching constant (K_{SV}) of 2.5×10^4 M^{-1} is acquired from the linear concentration dependency and this K_{SV} is similar to that of $PC_{61}BM$ ($K_{SV} = 1.6 \times 10^4$ M^{-1}).[28] Accordingly, we demonstrate electron-transfer from P3HT to DIR-2EH is as efficient as that to $PC_{61}BM$ in solution.

Using DIR-2EH as an electron acceptor in BHJ OSCs was tested with classical electron donor polymer P3HT in the fabricated device, ITO/PEDOT:PSS/P3HT:DIR-2EH/Ca/Al. Details of device fabrication and characterization are provided in ESI†. P3HT was blended with DIR-2EH in three different D/A ratios, 1:1, 1:2, and 1:4, to optimize condition for BHJ OSCs. The P3HT device using $PC_{61}BM$ as the electron acceptor material with 1:1 blending ratio was also fabricated as the reference device. As shown in Table 1 and Fig. 3, all devices based on DIR-2EH exhibit relatively high V_{OC} larger than 1.2 V, which is more than twice of the P3HT device using $PC_{61}BM$ (V_{OC} = 0.6 V) as the electron acceptor material. As demonstrated by the CV data, the higher V_{OC} can be mainly attributed to the much higher LUMO level of DIR-2EH than $PC_{61}BM$. This high V_{OC} value obtained from DIR-2EH is among the highest values reported for non-tandem BHJ OSCs.[24,26] Whereas V_{OC} and fill factors (*FF*s) remain mostly unchanged, the PCEs of

P3HT:DIR-2EH devices are susceptible to J_{SC}, which is closely related to the P3HT:DIR-2EH blending ratio.

Table 1 Device performance of P3HT:DIR-2EH BHJ OSCs.

Acceptor	D/A ratio	V_{OC} [V]	J_{SC} [mA/cm^2]	*FF* [%]	PCE [%]	R_S [Ω*cm^2]
DIR-2EH	1:1	1.24	2.64	59.3	1.94	481.2
	1:2	1.23	3.81	59.9	2.81	363.3
	1:4	1.22	4.29	58.2	3.05	275.9
$PC_{61}BM$	1:1	0.60	8.47	68.4	3.48	3.0

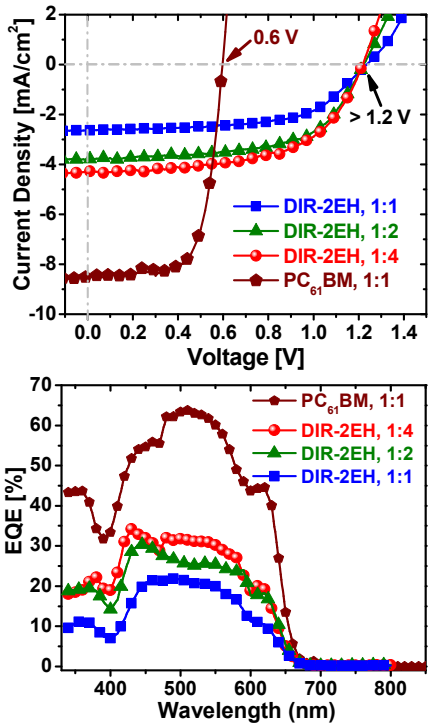

Fig. 3 *J-V* curves (top) and EQE spectra (bottom) of P3HT:DIR-2EH and P3HT:PC_{61}BM BHJ OSCs with different D/A ratios.

The external quantum efficiency (EQE) tracks the origin of J_{SC} in devices. From the EQE spectra of P3HT:DIR-2EH devices, the magnitude of EQE steadily enhanced with increasing DIR-2EH ratios and similar trend was observed for the corresponding J_{SC}s. Moreover, all DIR-2EH based devices exhibit EQE peaked around 420~470 nm that is different from ~510 nm of the device based on $PC_{61}BM$ electron acceptor. Considering the second reduction potential of CV, the rising EQE around 420~470 nm probably can be due to the absorption energy of charge transporting dianion state of DIR-2EH. Such EQE results indicate that DIR-2EH molecules photogenerate current not only absorb photons in BHJ OSCs.

The PCEs of P3HT:DIR-2EH BHJ OSCs improved with increasing DIR-2EH ratios. The optimum D/A ratio was 1:4 and achieved the best PCE of 3.05% with the highest short-circuit current density (J_{SC}) of 4.29 mA/cm^2, although such J_{SC} was just about half of that of P3HT:PC_{61}BM device. We believe that the much lower J_{SC} is unlikely due to the insufficient electron transfer or insufficient LUMO-LUMO offset between P3HT and DIR-2EH. First, the LUMO-LUMO offset is 0.5 eV (See Fig. 2 right), which is sufficiently large for the charge separation of P3HT exciton.[35] Second, a high PCE all polymer solar cell with very small LUMO-LUMO offset (< 0.1 eV) between donor and acceptor has been reported recently.[36] On the other hand, the lower J_{SC} could be attributed to the poor carrier selectivity at outer contacts of devices (e.g., highly donor-rich phase attaching the cathode surface), which could also result both lower FF and higher R_S in BHJ OPV devices.[37] As known or demonstrated for P3HT:PC_{61}BM BHJ OSCs, PC_{61}BM has a preferential tendency of bottom distribution,[38] which is probably no such tendency in P3HT:DIR-2EH BHJ OSC.

Similar to the reverse trend of J_{SC}, the *R*s steadily decreased with increasing D/A ratios, manifesting better charge transport is attainable with higher DIR-2EH content in P3HT thin film. Accordingly, we use the space-charged-limit-current (SCLC) method (details are in ESI†) to assess the charge transport property of P3HT:DIR-2EH blended thin film. The 1:4 blended thin film of P3HT:DIR-2EH showed an electron mobility of 1.26×10^{-8} m^2 V^{-1} s^{-1}, which is substantially higher than 6.89×10^{-9} m^2 V^{-1} s^{-1} of 1:1 blended thin film. However, the electron mobility of P3HT:DIR-2EH (1:4) blend is more than one order lower than 1.99×10^{-7} m^2 V^{-1} s^{-1} of P3HT:PC_{61}BM (1:1) blend based on our SCLC measurements. Inferior electron mobility may be one of the reasons for the much lower J_{SC} of P3HT:DIR-2EH than P3HT:PC_{61}BM devices.

Regarding the higher DIR-2EH content shows the better PCE, it is evident from morphology study. Fig. 4 shows the AFM images of P3HT:DIR-2EH blend thin film with three different DIR-2EH ratios and the blend thin film of P3HT:PC_{61}BM (1:1). The P3HT:DIR-2EH images exhibit less small-size agglomerates with increasing DIR-2EH content. It is interesting to note that the morphology of P3HT:DIR-2EH blend thin film with higher DIR-2EH ratios is getting closer to the morphology of P3HT:PC_{61}BM blend thin film. A larger size of agglomerates may afford a longer bicontinuous charge transport channels and a less grain boundary that is obstacle to charge transport. The morphology observation is consistent with the electron mobility estimated by SCLC and EQE spectra, J_{SC} and R_S of fabricated BHJ OSCs.

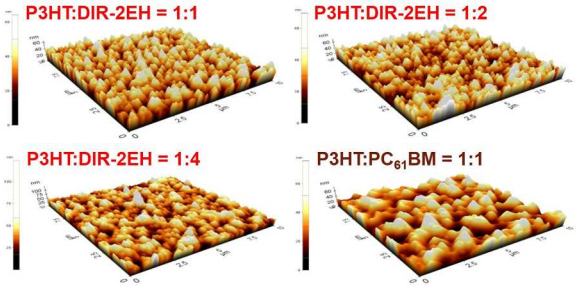

Fig. 4 AFM Images (10 × 10 μm) of blend thin films based on P3HT:DIR-2EH (1:1, 1:2, 1:4) or P3HT:PC_{61}BM (1:1).

In conclusion, we report a novel all-carbon non-fullerene electron acceptor material based on diindeno[1,2-*g*:1',2'-*s*]rubicene (DIR) for the application of BHJ OSCs. This novel electron acceptor material exhibits a high LUMO level, which results a relatively high V_{OC} larger than 1.2 V in P3HT-based BHJ OSCs. Device's electrical properties of J_{SC} and *Rs*, electron mobility of blended thin film, and the thin film morphology all have been demonstrated susceptible to the blend ratios of P3HT:DIR-2EH. The device with the highest ratio of 1:4 yielded the best PCE of 3.05%, which is one of few P3HT-based non-fullerene BHJ OSCs having PCE over 3%.[18,39] Our results have demonstrated that easily synthesized and processed rubicene is a promising core structure for the development of high performance non-fullerene electron acceptor materials used in BHJ OSCs.

Notes and references

[a] *Institute of Chemistry, Academia Sinica, Taipei, Taiwan 11529, Republic of China. Fax:+886 2 27831237; Tel:+886 2 27898542;*
E-mail: chintchen@gate.sinica.edu.tw
[b] *Department of Chemistry, National Taiwan University, Taipei, Taiwan 10617.*

† Electronic Supplementary Information (ESI) available: Experimental details of syntheses and characterizations. See DOI: 10.1039/c000000x/

1. J. You, L. Dou, K. Yoshimura, T. Kato, K. Ohya, T. Moriarty, K. Emery, C.-C. Chen, J. Gao, G. Li, and Y. Yang, *Nat. Commun.*, 2013, **4**, 1446.
2. Y. Liu, C.-C. Chen, Z. Hong, J. Gao, Y. M. Yang, H. Zhou, L. Dou, G. Li, and Y. Yang, *Sci. Rep.*, 2013, **3**, 3356.
3. Y. He and Y. Li, *Phys. Chem. Chem. Phys.*, 2011, **13**, 1970–1983.
4. A. Anctil, C. W. Babbitt, R. P. Raffaelle, and B. J. Landi, *Environ. Sci. Technol.*, 2011, **45**, 2353–2359.
5. F. E. Ala'a, J.-P. Sun, I. G. Hill, and G. C. Welch, *J. Mater. Chem. A*, 2014, **2**, 1201–1213.
6. Y. Lin and X. Zhan, *Mater. Horiz.*, 2014, **1**, 470–488.
7. Y. Kim and E. Lim, *Polymers*, 2014, **6**, 382–407.
8. X. Zhang, Z. Lu, L. Ye, C. Zhan, J. Hou, S. Zhang, B. Jiang, Y. Zhao, J. Huang, S. Zhang, Y. Liu, Q. Shi, Y. Liu, and J. Yao, *Adv. Mater.*, 2013, **25**, 5791–5797.
9. Y. Zang, C.-Z. Li, C. C. Chueh, S. T. Williams, W. Jiang, Z.-H. Wang, J.-S. Yu, and A. K. Y. Jen, *Adv. Mater.*, 2014, **26**, 5708–5714.
10. Y. Lin, Y. Wang, J. Wang, J. Hou, Y. Li, D. Zhu, and X. Zhan, *Adv. Mater.*, 2014, **26**, 5137–5142.
11. R. Shivanna, S. Shoaee, S. Dimitrov, S. K. Kandappa, S. Rajaram, J. R. Durrant, and K. S. Narayan, *Energy Environ. Sci.*, 2014, **7**, 435–441.
12. W. Jiang, L. Ye, X. Li, C. Xiao, F. Tan, W. Zhao, J. Hou, and Z. Wang, *Chem. Commun.*, 2014, **50**, 1024–1026.
13. Y. Zhong, M. T. Trinh, R. Chen, W. Wang, P. P. Khlyabich, B. Kumar, Q. Xu, C.-Y. Nam, M. Y. Sfeir, C. Black, M. L. Steigerwald, Y.-L. Loo, S. Xiao, F. Ng, X. Y. Zhu, and C. Nuckolls, *J. Am. Chem. Soc.*, 2014, **136**, 15215–15221.
14. Y. Zhou, L. Ding, K. Shi, Y.-Z. Dai, N. Ai, J. Wang, and J. Pei, *Adv. Mater.*, 2012, **24**, 957–961.
15. Y. Lin, Y. Li, and X. Zhan, *Adv. Energy Mater.*, 2013, **3**, 724–728.
16. Y. Fang, A. K. Pandey, A. M. Nardes, N. Kopidakis, P. L. Burn, and P. Meredith, *Adv. Energy Mater.*, 2013, **3**, 54–59.
17. J. T. Bloking, X. Han, A. T. Higgs, J. P. Kastrop, L. Pandey, J. E. Norton, C. Risko, C. E. Chen, J.-L. Brédas, and M. D. McGehee, *Chem. Mater.*, 2011, **23**, 5484–5490.
18. Z. Mao, W. Senevirathna, J.-Y. Liao, J. Gu, S. V. Kesava, C. Guo, E. D. Gomez, and G. Sauvé, *Adv. Mater.*, 2014, **26**, 6290–6294.
19. H. Xia, D. Liu, X. Xu, and Q. Miao, *Chem. Commun.*, 2013, **49**, 4301–4303.
20. H. Dang, M. Levitus, and M. A. Garcia-Garibay, *J. Am. Chem. Soc.*, 2002, **124**, 136–143.
21. D. T. Chase, A. G. Fix, S. J. Kang, B. D. Rose, C. D. Weber, Y. Zhong, L. N. Zakharov, M. C. Lonergan, C. Nuckolls, and M. M. Haley, *J. Am. Chem. Soc.*, 2012, **134**, 10349–10352.
22. M. Nakano, I. Osaka, K. Takimiya, and T. Koganezawa, *J. Mater. Chem. C*, 2013, **2**, 64–70.
23. A. R. Mohebbi, J. Yuen, J. Fan, C. Munoz, M. F. Wang, R. S. Shirazi, J. Seifter, and F. Wudl, *Adv. Mater.*, 2011, **23**, 4644–4648.
24. F. G. Brunetti, X. Gong, M. Tong, A. J. Heeger, and F. Wudl, *Angew. Chem. Int. Ed.*, 2010, **49**, 532–536.
25. X. Gong, M. Tong, F. G. Brunetti, J. Seo, Y. Sun, D. Moses, F. Wudl, and A. J. Heeger, *Adv. Mater.*, 2011, **23**, 2272–2277.
26. H. U. Kim, J.-H. Kim, H. Suh, J. Kwak, D. Kim, A. C. Grimsdale, S. C. Yoon, and D.-H. Hwang, *Chem. Commun.*, 2013, **49**, 10950–10952.
27. O. Y. Park, H. U. Kim, J.-H. Kim, J. B. Park, J. Kwak, W. S. Shin, S. C. Yoon, and D.-H. Hwang, *Sol. Energy Mater. Sol. Cells*, 2013, **116**, 275–282.
28. J. D. Wood, J. L. Jellison, A. D. Finke, L. Wang, and K. N. Plunkett, *J. Am. Chem. Soc.*, 2012, **134**, 15783–15789.
29. J. L. Jellison, C.-H. Lee, X. Zhu, J. D. Wood, and K. N. Plunkett, *Angew. Chem. Int. Ed.*, 2012, **51**, 12321–12324.
30. L. Ye, H. Xia, Y. Xiao, J. Xu, and Q. Miao, *RSC Adv.*, 2014, **4**, 1087–1092.
31. H. Lee, Y. Zhang, L. Zhang, T. Mirabito, E. K. Burnett, S. Trahan, A. R. Mohebbi, S. C. Mannsfeld, F. Wudl, and A. L. Briseno, *J. Mater. Chem. C*, 2014, **2**, 3361–3366.
32. M. Bown, C. J. Dunn, C. M. Forsyth, P. Kemppinen, T. B. Singh, M. A. Skidmore, and K. N. Winzenberg, *Aust. J. Chem.*, 2012, **65**, 145–152.
33. B. Scherwitzl, W. Lukesch, A. Hirzer, J. Albering, G. Leising, R. Resel, and A. Winkler, *J. Phys. Chem. C*, 2013, **117**, 4115–4123.
34. J. Hou, T. L. Chen, S. Zhang, L. Huo, S. Sista, and Y. Yang, *Macromolecules*, 2009, **42**, 9217–9219.
35. J. D. Servaites, M. A. Ratner, and T. J. Marks, *Energy Environ. Sci.*, 2011, **4**, 4410–4422.
36. Y. Zhou, T. Kurosawa, W. Ma, Y. Guo, L. Fang, K. Vandewal, Y. Diao, C. Wang, Q. Yan, J. Reinspach, J. Mei, A. L. Appleton, G. I. Koleilat, Y. Gao, S. C. B. Mannsfeld, A. Salleo, H. Ade, D. Zhao, and Z. Bao, *Adv. Mater.*, 2014, **26**, 3767–3772.
37. A. Guerrero, B. Dörling, T. Ripolles-Sanchis, M. Aghamohammadi, E. Barrena, M. Campoy-Quiles, and G. Garcia-Belmonte, *ACS Nano*, 2013, **7**, 4637–4646.
38. Z. Xu, L.-M. Chen, G. Yang, C.-H. Huang, J. Hou, Y. Wu, G. Li, C.-S. Hsu, and Y. Yang, *Adv. Funct. Mater.*, 2009, **19**, 1227–1234.
39. Y. Kim, C. E. Song, S.-J. Moon, and E. Lim, *Chem. Commun.*, 2014, **50**, 8235–8238.

Table of Contents